COBEM 2023 27TH INTERNATIONAL CONGRESS OF MECHANICAL ENGENEERING

ABCM Brazilian Society of Mechanical Sciences and Engineering
27th ABCM International Congress of Mechanical Engineering
December 04-08, 2023, Florianópolis-SC, Brazil

COB-2023-1444
17-4 PH STAINLESS STEEL DEPOSITED BY THE METALLIC FUSED FILAMENT FABRICATION (FFF) PROCESS

Júlia Fornaziero de Almeida
Fábio Edson Mariani
Department of Production Engineering, São Carlos School of Engineering, University of São Paulo, Av. Trabalhador São-Carlense, 400 – Parque Arnold Schimidt, São Carlos, 13566-590, Brazil
julia.f.almeida@usp.br; mariani.fabioe@gmail.com

Raul Molina Jeronymo
Indigo-de, São Carlos, St. Conde do Pinhal, 1762 – Nucleo Res. Silvio Vilari, São Carlos, 13560-648, Brazil
r.jeronymo@indigo-de.com

Reginaldo Teixeira Coelho
Department of Production Engineering, São Carlos School of Engineering, University of São Paulo, Av. Trabalhador São-Carlense, 400 – Parque Arnold Schimidt, São Carlos, 13566-590, Brazil
rtcoelho@sc.usp.br

Abstract. *The Material Extrusion Process, Fused Filament Fabrication (FFF) for metals, has as its principle the use of filament composed of polymer binders and metal alloy in powder form. During the metal FFF, the composite filament is melted and deposited in successive layers to produce a geometry. After the construction, the part is submitted to the debinding and sintering processes to obtain a solid structure. Compared to other metal AM processes, the FFF is an alternative, easier to operate, and cost-effective. However, this process still needs studies to achieve consolidated mechanical properties. Many parameters influence the quality of the final part produced by the FFF, and these depend directly on the specifications of the used materials. Based on this perspective, this work aimed to produce and characterize a sample of 17-4 PH stainless steel deposited using metallic FFF process. We performed volumetric analyses using a 3D scanner and characterized the sample using confocal laser microscopy, Scanning Electron Microscopy (SEM), X-ray Energy Dispersive Spectroscopy (EDX), Vickers microhardness, and calotest microadhesive wear test. A sample with chemical compositions similar to casting 17-4 PH steel was obtained. The hardness and wear results showed similarities between the deposited sample, indicating efficiency in the deposition parameters.*

Keywords: *Additive Manufacturing, Material Extrusion Process, Fused Filament Fabrication, Metal, Material Characterization.*

1. INTRODUCTION

Material Extrusion (ME) is the Additive Manufacturing (AM) process that is most used worldwide. The FFF (Fused Filament Fabrication) is one of the ME processes “in which material is selectively dispensed through a nozzle or orifice” (ISO/ASTM 52900, 2015). Although commonly used for polymers, such as Polylactic Acid (PLA), Acrylonitrile Butadiene Styrene (ABS), or Polyethylene terephthalate glycol (PETG), these processes can also produce metallic components.

In comparison, Powder Bed Fusion, and Directed Energy Deposition, are the most advanced processes for metal applications (Bourell et al., 2017; Calignano et al., 2019), but both are expensive (Atzeni and Salmi, 2012; Niaki and Nonino, 2017). Due to this status quo, the search for new solutions in processes more accessible, like FFF, became attractive to the industry.

The 17-4 PH is one of the most used stainless-steel materials. It can be used for applications in petrochemistry, aerospace, aviation, automotive, and the medical industry, being ideal for components within corrosive environments that require high mechanical strength and hardness (Sculpteo, 2023). Was the first non-polymeric material that was successfully fabricated using metal FFF with high-dimension accuracy and precision (Suwanpreecha et al., 2021; Suwanpreecha and Manonukul, 2022).

Parts made by Metal FFF (MFFF) need Debinding and Sintering (D&S) processes, the same provided for Metal Injection Molding (MIM) procedure. However, up to now, these parts cannot replace direct metal AM or conventional manufacturing but can be an alternative to other areas for rapid tooling or functional prototyping (Lavecchia et al., 2023). The applicability of the MFFF process is scarce for pure metal components (Pragana et al., 2021), which requires more

studies to analyze the feedstock performance. Also, even with new commercialized metal filaments for FFF combining polymer and metal powder, only a few companies in Brazil provide D&S processes.

Most of the studies focus on as-printed properties and printing parameters, while only a few analyses consider sintered physical and mechanical properties of metal FFF (Suwanpreecha et al., 2021). For this reason, continuous research about this material is important to achieve new areas and provide metal parts with low costs.

This paper aimed to analyze a sample of 17-4 PH stainless steel deposited through the metallic FFF process. We performed both macro and micro analyses. The macro analysis used a 3D scanner to verify the printing process's quality and the sample shrinkage after the debinding and sintering. The microanalysis focused on characterizing the sample using confocal laser microscopy, Scanning Electron Microscopy (SEM), X-ray energy dispersive spectroscopy (EDX), Vickers microhardness and calotest micro adhesive wear test.

2. ADDITIVE MANUFACTURING

Additive Manufacturing (AM), also known as 3D printing, has become one of the emergent technologies impacting several industrial sectors. Is defined as a "process of joining materials to make parts from 3D model data, usually layer upon layer, as opposed to subtractive manufacturing and formative manufacturing methodologies" (ISO/ASTM 52900, 2015). Seven processes are recognized by the standard ISO/ASTM 52900 (2015): Binder Jetting (BJ); Directed Energy Deposition (DED); Material Extrusion (ME); Material Jetting (MJ); Powder Bed Fusion (PBF); Sheet Lamination (SL); and Vat Photopolymerization (VP). Four of those processes (PBF, DED, BJ, and SL) are used for direct metallic application (Pragana et al., 2021; Strong et al., 2018) and are known as Direct Metal Additive Manufacturing (MAM). The other processes (VP, MJ, and ME) are mainly used for indirect MAM (Pragana et al., 2021). In this study, we focused on metallic Material Extrusion.

2.1 Metallic Material Extrusion

For metallic Material Extrusion, two processes were combined: FFF and MIM. MIM is a traditional process that provides almost fully dense metal parts combining injection molding, Debinding and Sintering (D&S) processes (Lavecchia et al., 2023). Materials for this application have been commercialized by companies such as BASF.

After the FFF printing stage is finished, a "Green Part" is obtained. This printing undergoes a debinding process to remove the polymer binding agent. The part obtained after the debinding ("Brown Part") is porous and requires a sintering process to acquire a solid, dense geometry ("White Part"). After that, to achieve the desired quality additional post-processing such as polishing, milling, heat-treatment, or coating can be performed (Lavecchia et al., 2023; Sculpteo, 2023). Figure 1 shows the metal FFF process as suggested by BASF.

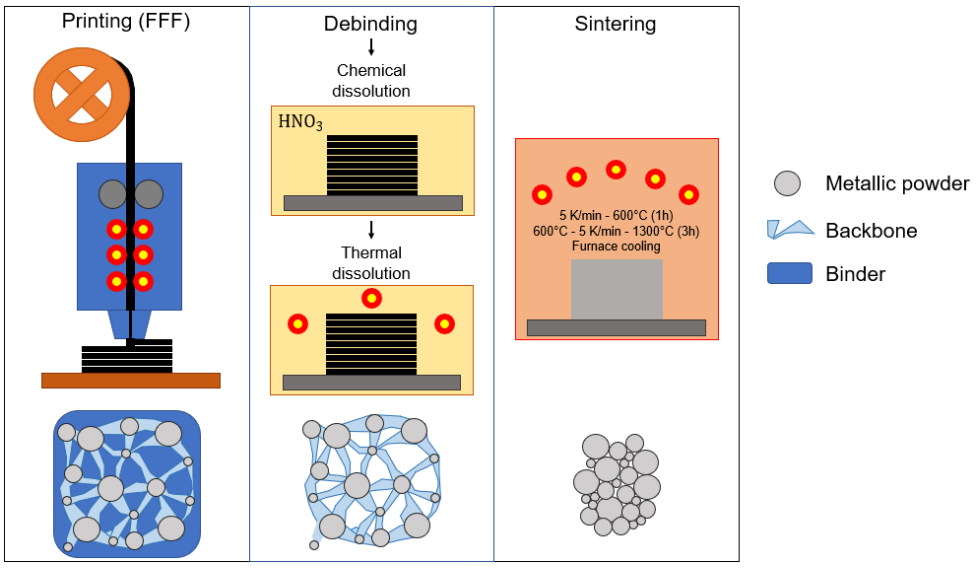

Figure 1. Metal FFF process. Adapted from Boschetto et al. (2022), considering the recommended parameters provided by BASF (2023) for 17-4 PH.

The debinding step is needed to remove the polymeric binder from the part. The sintering process burns the remaining binder and then consolidates the piece (Lavecchia et al., 2023). The as-sintered part is significantly smaller than the as-printed part; this phenomenon happens because of the consolidation of the metal powder during sintering after the polymer binders were removed from the debinding process (Suwanpreecha and Manonukul, 2022).

One material available for the MFFF process is the 17-4 PH, a chromium-copper martensitic precipitation-hardened stainless steel. This material is magnetic, fully heat treatable to high levels of strength and hardness and maintains its mechanical and corrosion resistance at temperatures up to 315 °C (600 °F). The feedstock of 17-4 PH metal filament is made of a polymer matrix (Polyoxymethylene (POM) 1 Polypropylene (PP)) and stainless-steel powder (17-4 PH) (Sculpteo, 2023).

The benefits of using a metal filament like the Ultrafuse 17-4 PH are: the filament is an easy and affordable way of metal 3D printing using the FFF process, presents high mechanical strength and hardness and has good corrosion strength (Sculpteo, 2023). Some applications are presented by BASF, such as a spare part solar panel clamp (Figure 2A) and a customized tool insert (Figure 2B).

Figure 2. Metal parts produced by metal FFF (BASF, 2023)

3. METHODOLOGY

The filament BASF Ultrafuse 17-4 PH was used for printing a rectangular sample on a commercial printer, and the debinding and sintering were performed by a third party following the BASF parameters recommendation. The sample was printed with an infill of 100%, with dimensions of 48 x 24 x 12.6 mm.

We performed both macro analyses and microanalysis of the sample. The macro involved two volumetric inspection analyses using an optical 3D Scanner, which, as explained by Wevolver (2022), produces a mesh or a point cloud, providing all the needed dimensional information about the surface of the geometry. The first inspection compared the CAD against the Green Parts to check for any volumetric problems within the printing process. The second inspection was to confirm if the results of the parts obtained after the D&S achieved the target's dimensions (calculated through the ratios recommended by the filament manufacturers).

For the coatings cross-section analyses, the metallographic preparation involved conventional cutting (using a diamond abrasive disk), embedding in Bakelite, sanding with SiC sandpaper up to 1500 mesh, and polishing with aqueous alumina solutions of 1.00, 0.25, and 0.05 µm. The sample was then analyzed using Confocal Laser Scanning Microscopy (CLSM), Scanning Electron Microscopy (SEM), and X-ray Energy-Dispersive Spectroscopy (EDX). For calculations of the percentage of voids, the standard ASTM E1245-E03 was used and applied to the images produced by the CLSM. Vickers Microhardness (HV) tests were performed to obtain the average hardness. Twenty measurements were taken to calculate the mean and standard deviation. A load of 10.0 N was applied with a dwell time of 15 s.

4. RESULTS AND DISCUSSION

Before the printing process started, a quality check was performed on the bought filament to avoid problems such as chemical variations, a possibility due to the being a different marketed product to the bibliographical reference ones. Figure 3 shows a cross-section of the BASF Ultrafuse 17-4 PH filament.

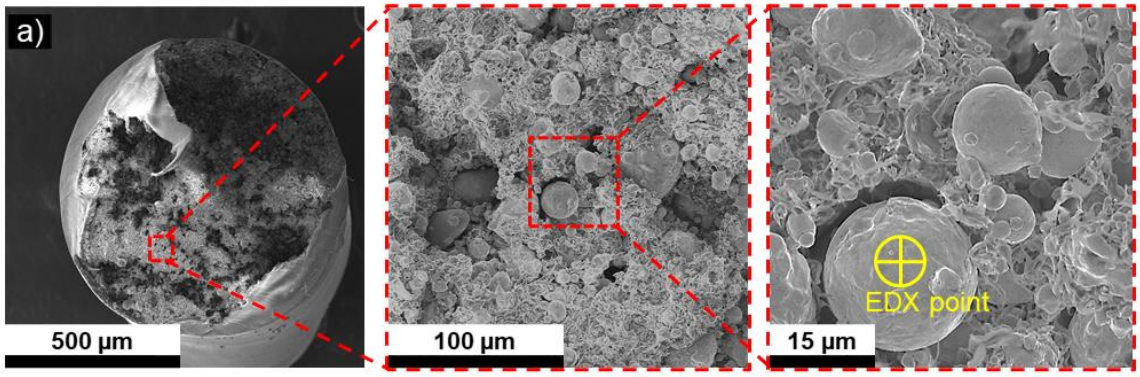

b)

EDX point - Chemical composition (wt%)						
Fe	Cr	Ni	Cu	Si	Mn	Nb
73.2	17.3	3.6	3.3	0.8	0.6	0.3

Figure 3. (a) SEM and (b) EDX analysis of the cross-section of the filament used to produce the sample.

The analysis used was Scanning Electron Microscopy (SEM), verifying that the filament is composed of spherical particles with a chemical composition similar to that of 17-4 PH steel presented in Lavecchia et al. (2023). The particle sizes vary between 10 and 20 µm.

Figure 4 shows the sample after the debinding and sintering processes.

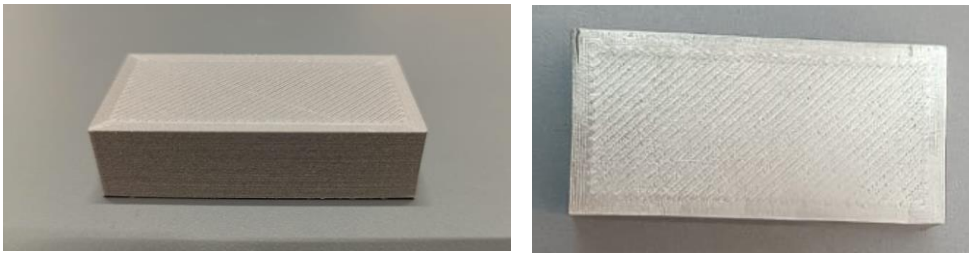

Figure 4. a) Sample obtained after the FFF printing (Green Part); b) Sample obtained after the D&S (White Part).

The shrinkage is attributed to the high-volume percentage of binder in the Green Part (as much as 50%). During sintering, a large shrinkage occurs. Therefore, it is essential to ensure that shrinkage is controlled during the sintering process (Rane and Strano, 2019). However, as seen through the first analysis (Figure 5), the printed components already had some deviation compared with their CAD counterpart.

The analysis indicates warping, a common problem of the FFF process that usually happens due to the difference in temperature between the heated bed and the part. It affected the entire base of the sample, but it is more visible at the bottom left, where the deviation surpassed 0.31 mm against its intended volume. Due to this extra material in the base, the middle of the left side shrinks, reaching -0.15 mm.

Besides the warping, the part presented less material at the top, peaking at -0.12 mm. This issue might be related to the finishing process, included in the top layers of the printing, when the nozzle presses itself against the deposited material, generating a more polished surface. Because of the pressure applied to the surface, there is a chance that less material is deposited in the top, which depends on the viscosity of the filament.

Both issues didn't hinder the following steps, so we proceeded with the D&S processes. However, we noted that the effects of the warping issue persisted even in the geometry of the White Part, which could prevent real applications for the component.

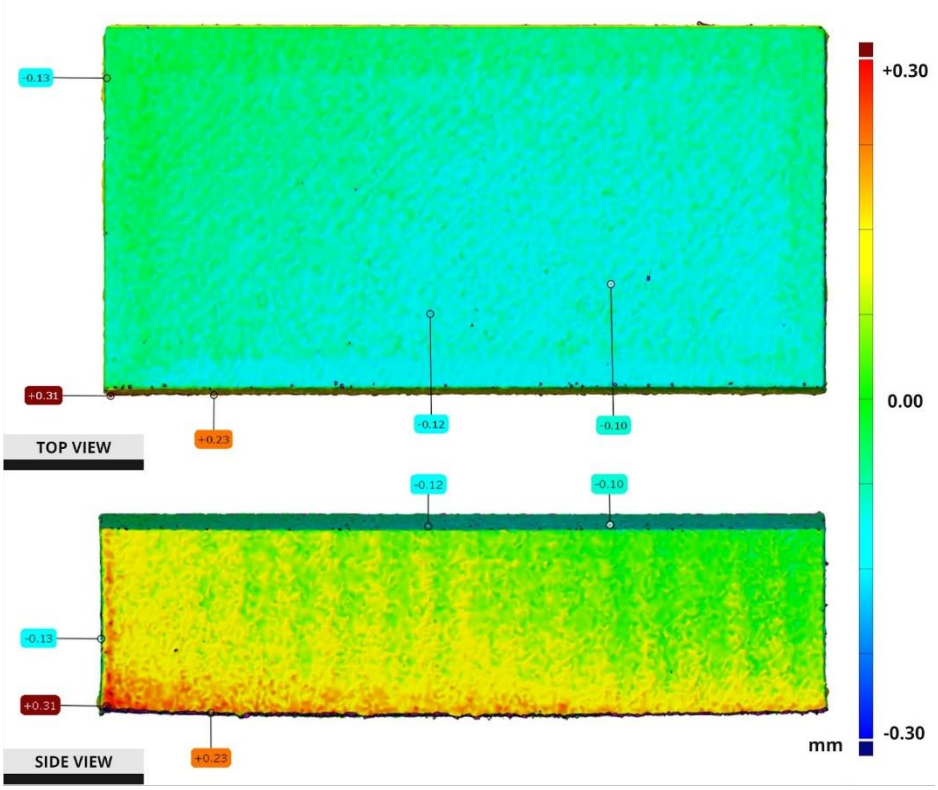

Figure 5. (a) Volumetric inspection of the sample's Green Part against its CAD.

There are suggested ratios to correct the shrinkage of the post-sintered parts, including guidelines from the filament manufacturer. However, since the geometry of the printed part influences the shrinkage, it may require customized ratios for each project to reach more accurate results. Advanced tools to anticipate shrinkage ratios are also used, including prediction through Finite Elements Simulation (Heaney and Spina, 2007).

For this analysis, we used the average factor provided by (BASF, 2023), which revolves around 20% shrinkage in the XY axis and 26% in the Z axis, which is why the 3D model was escalated from 40.00 x 20.00 x 10.00mm to 48.00 x 24.00 x 12.60mm.

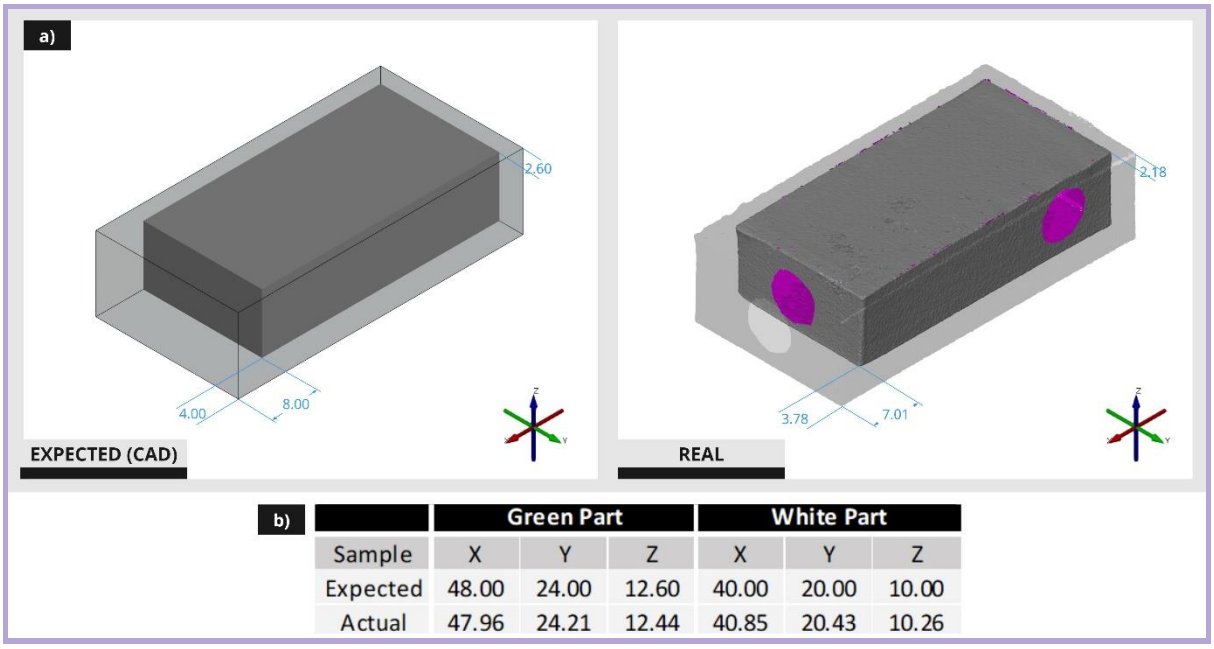

	Green Part			White Part		
Sample	X	Y	Z	X	Y	Z
Expected	48.00	24.00	12.60	40.00	20.00	10.00
Actual	47.96	24.21	12.44	40.85	20.43	10.26

Figure 6. (a) Size comparison of actual "Green" and "White" parts. The pink area represents the 3D scanner's "guides" and thus was not considered in the analysis; (b) Expected sizes against actual sample (in millimetres).

Figure 6 shows the correlation between the expected shrinkage (left side) and the average of the actual reduction (right side) captured through the 3D scanner. According to the analysis, the average shrinkage of the real geometry was 14.65% on the X-axis, 15.61% on the Y-axis and 17.72% on the Z-axis. Expressly, all the real shrinkages were lower than the expected ratios, almost reaching 1 mm of difference on the X-axis.

Entering the micro analysis, Figure 7 shows the confocal laser micrograph of the cross-sectional area.

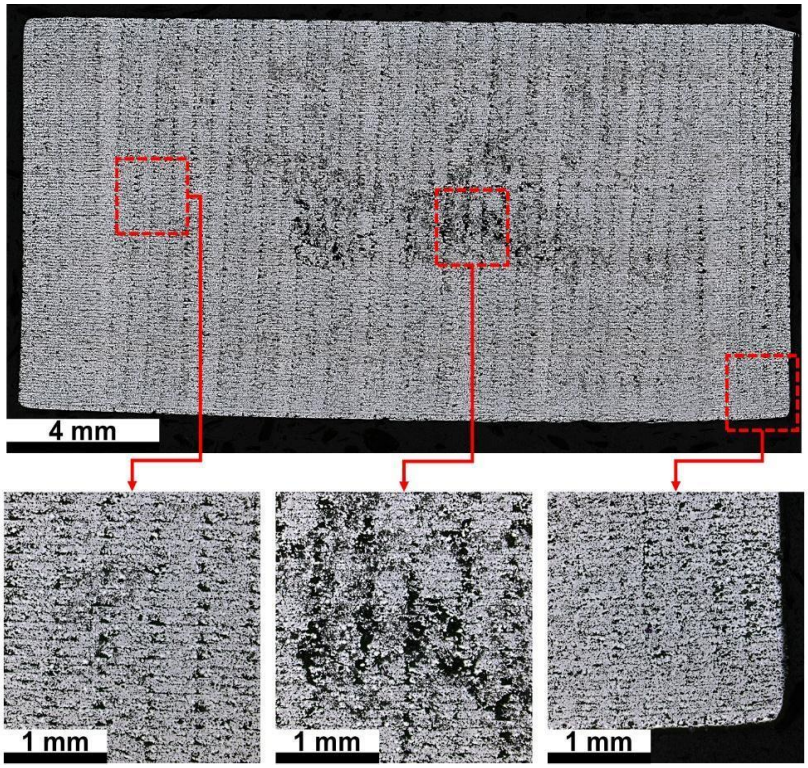

Figure 7. Confocal laser micrograph of the sample after the Debinding and Sintering processes.

The presence of voids is observed throughout the entire perimeter of the cross-sectional area, with a more significant concentration in the central region. These results indicate that the sintering parameters were not sufficiently effective to ensure the complete filling of the sample. Quantitative analyses conducted through laser confocal microscopy indicated that 71.3% of the cross-sectional area was satisfactorily filled, with a hardness of 230 ± 18 HV_{10}. As provided by BASF, the filament manufacturer, the hardness of the constructed part after sintering is 291 HV_{10} (BASF, 2023), a value lower than that obtained in this study. The low hardness value observed in the produced piece is associated with the quantity of voids present in the sample. It is believed that this porosity may have resulted either from inadequate control of the 3D printing parameters during the manufacturing process or an ineffective sintering process. For future optimizations, it will be essential to verify these parameters to achieve a part with higher density and, consequently, higher hardness, according to the project's needs and specifications.

Figure 8 presents the Scanning Electron Micrograph (SEM), along with the chemical mapping obtained through EDX, conducted on the cross-sectional area of the sample.

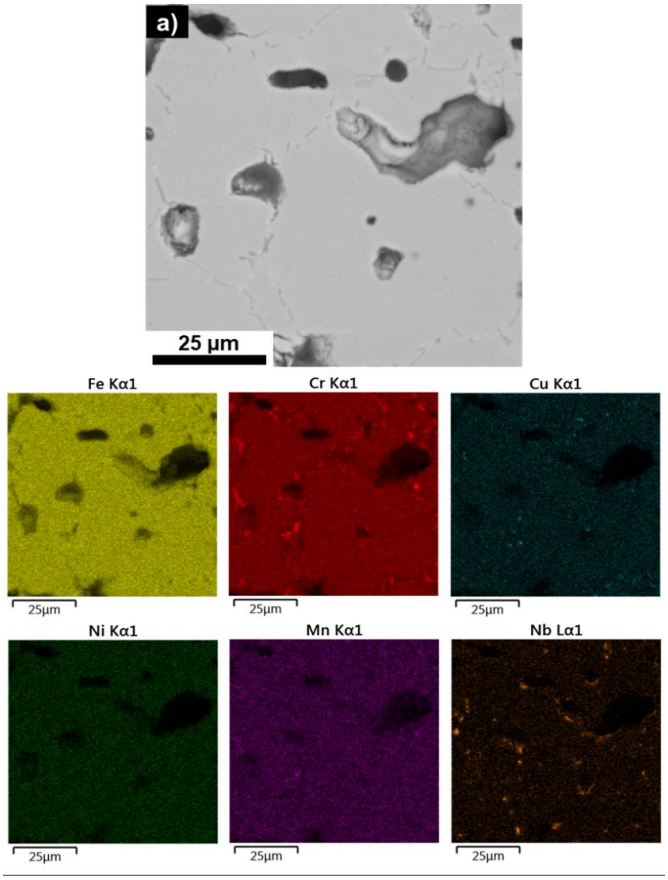

b)

Chemical composition (wt%)						
Fe	Cr	Ni	Cu	Si	Mn	Nb
73.7	17.4	3.9	3.5	0.8	0.4	0.3

Figure 8. (a) SEM and EDX mapping conducted on the sample. (b) Quantitative EDX analysis, performed on the mapped area.

The elements Fe, Cr, Cu, Ni, and Mn are distributed throughout the analyzed region, while Nb shows higher clustering in specific areas (Figure 8a). Other studies have reported similar EDX results (Lavecchia et al., 2023; Suwanpreecha et al., 2021).

The EDX analysis did not indicate the presence of the chemical element O. In other studies, the presence of O was observed in the as-built sample, and it was correlated with the $MnCr_2O_4$ phase, which was obtained during the processing of the raw material (Suwanpreecha et al., 2021).

The results of the quantitative EDX analysis (Figure 8b) indicate that the sample's chemical composition resembles that of 17-4 PH steel produced through the conventional casting process (Lavecchia et al., 2023).

5. CONCLUSION

The results of the analysis indicate that the chemical composition of the sample resembles that of 17-4 PH steel produced through conventional casting, which suggests that the 3D-printed part has achieved a comparable composition. However, the presence of voids throughout the cross-sectional area, particularly in the central region, indicates that the sintering parameters were not entirely effective in ensuring the complete filling of the sample.

The distribution of elements Fe, Cr, Cu, Ni, and Mn is uniform throughout the analyzed region, while Nb shows higher clustering in specific areas. This suggests that the 3D printing process has successfully incorporated these elements.

The macro analysis showed that volumetric deviations were already present in the "Green Part" and persisted through the D&S, providing that the 3D printing process requires better settings for end-part productions. Additionally, we observed that the sample shrank less than the expected ratio informed by the manufacturer, which opens space for further research on the topic since the cause can be related to the shrinking ratios applied on the 3D printing or the temperature control of the D&S processes. Likewise, both volumetric issues could be solved with additional machining, ensuring the required accuracy.

The quantitative EDX analysis revealed that approximately 71.3% of the cross-sectional area was satisfactorily filled, resulting in a hardness of 230 ± 18 HV. However, this hardness value is lower than the one reported by the filament manufacturer BASF, which indicates that the presence of voids has significantly affected the overall hardness of the produced part.

To enhance future 3D printing optimizations, it will be crucial to address the issue of porosity by improving the control of the printing parameters or guaranteeing the sintering efficiency. This improvement will lead to higher density and increased hardness, aligning with the project's requirements and specifications. By addressing these aspects, it is possible to achieve 3D-printed parts with improved mechanical characteristics, closer to those of conventionally produced 17-4 PH steel, expanding the potential applications of additive manufacturing in various industries.

Additionally, a comparison with other metal AM processes and a discussion on the limitations and future directions of FFF for metal printing could have further enriched the paper

6. ACKNOWLEDGEMENTS

We thank the company Indigo Design Engineering for the partnership in this project.

7. REFERENCES

Atzeni, E., and Salmi, A., 2012. Economics of additive manufacturing for end-usable metal parts. The International Journal of Advanced Manufacturing Technology, 62(9–12), 1147–1155. https://doi.org/10.1007/s00170-011-3878-1

BASF, 2023. Ultrafuse® 17-4 PH Metal Filament for 3D Printers. BASF Forward AM. https://forward-am.com/material-portfolio/ultrafuse-filaments-for-fused-filaments-fabrication-fff/metal-filaments/ultrafuse-17-4-ph/

Boschetto, A., Bottini, L., Miani, F., and Veniali, F., 2022. Roughness investigation of steel 316L parts fabricated by Metal Fused Filament Fabrication. Journal of Manufacturing Processes, 81, 261–280. https://doi.org/10.1016/j.jmapro.2022.06.077

Bourell, D., Kruth, J. P., Leu, M., Levy, G., Rosen, D., Beese, A. M., and Clare, A., 2017. Materials for additive manufacturing. CIRP Annals, 66(2), 659–681. https://doi.org/10.1016/j.cirp.2017.05.009

Calignano, Galati, and Iuliano, 2019. A Metal Powder Bed Fusion Process in Industry: Qualification Considerations. Machines, 7(4), 72. https://doi.org/10.3390/machines7040072

Heaney, D. F., and Spina, R., 2007. Shrinkage prediction of MIM parts by finite element simulation. International Journal of Computational Materials Science and Surface Engineering, 1(1), 57. https://doi.org/10.1504/IJCMSSE.2007.013835

ISO/ASTM 52900, S., 2015. Standard Terminology for Additive Manufacturing – General Principles – Terminology.

Lavecchia, F., Pellegrini, A., and Galantucci, L. M., 2023. Comparative study on the properties of 17-4 PH stainless steel parts made by metal fused filament fabrication process and atomic diffusion additive manufacturing. Rapid Prototyping Journal, 29(2), 393–407. https://doi.org/10.1108/RPJ-12-2021-0350

Niaki, M. K., and Nonino, F., 2017. Impact of additive manufacturing on business competitiveness: a multiple case study. Journal of Manufacturing Technology Management, 28(1), 56–74. https://doi.org/10.1108/JMTM-01-2016-0001

Pragana, J. P. M., Sampaio, R. F. V., Bragança, I. M. F., Silva, C. M. A., and Martins, P. A. F., 2021. Hybrid metal additive manufacturing: A state–of–the-art review. Advances in Industrial and Manufacturing Engineering, 2, 100032. https://doi.org/10.1016/j.aime.2021.100032

Rane, K., and Strano, M., 2019. A comprehensive review of extrusion-based additive manufacturing processes for rapid production of metallic and ceramic parts. Advances in Manufacturing, 7(2), 155–173. https://doi.org/10.1007/s40436-019-00253-6

Sculpteo, 2023. BASF ultrafuse 17-4 PH. https://www.sculpteo.com/en/materials/fdm-material/ultrafuse-17-4-ph/

Strong, D., Kay, M., Conner, B., Wakefield, T., and Manogharan, G., 2018. Hybrid manufacturing – integrating traditional manufacturers with additive manufacturing (AM) supply chain. Additive Manufacturing, 21, 159–173. https://doi.org/10.1016/j.addma.2018.03.010

Suwanpreecha, C., and Manonukul, A., 2022. On the build orientation effect in as-printed and as-sintered bending properties of 17-4PH alloy fabricated by metal fused filament fabrication. Rapid Prototyping Journal, 28(6), 1076–1085. https://doi.org/10.1108/RPJ-07-2021-0174

Suwanpreecha, C., Seensattayawong, P., Vadhanakovint, V., and Manonukul, A., 2021. Influence of Specimen Layout on 17-4PH (AISI 630) Alloys Fabricated by Low-Cost Additive Manufacturing. Metallurgical and Materials Transactions A, 52(5), 1999–2009. https://doi.org/10.1007/s11661-021-06211-x

Wevolver, 2022. 3D Scanner for CAD : The Best 3D Scanners and Scan-to-CAD Softwares. Wevolver. https://www.wevolver.com/article/3d-scanner-for-cad-the-best-3d-scanners-and-scan-to-cad-softwares

8. RESPONSIBILITY NOTICE

The authors are the only responsible for the printed material included in this paper.